AIAA SciTech Forum
8-12 January 2024, Orlando, FL
AIAA SCITECH 2024 Forum

10.2514/6.2024-2827

Dual-Band Scanned-Wavelength Infrared Laser-Induced-Fluorescence Thermometry of CO

Garrett C. Mathews*, Jonathan Rustad†, and Christopher S. Goldenstein ‡
Purdue University, 585 Purdue Mall, West Lafayette, IN, 47907

Infrared laser-induced fluorescence (IR-LIF) enables spatially resolved measurements of stable chemical species (e.g., CO, CO_2) and gas properties via excitation of rovibrational transitions and detection of the resulting infrared fluorescence. This article presents a novel dual-band IR-LIF diagnostic that can provide gas temperature measurements via CO at measurement rates up to 1 kHz. The diagnostic utilizes a quantum-cascade laser (QCL) emitting near 2013.3 cm^{-1} and an optical parametric oscillator (OPO) emitting near 4297.7 cm^{-1} to sequentially scan across the P(0,30) transition in the fundamental vibrational band of CO and the R(0,10) transition in the first overtone band of CO, respectively. A model describing the IR-LIF signals in the time domain was developed and least-squares fit to the measured LIF signals to extract the integrated area, collisional-broadening full-width, and characteristic times of the LIF signal for each CO transition. The diagnostic was demonstrated with temperature measurements acquired at rates of 100 Hz and 1 kHz in a CO-H_2-Ar diffusion flame at atmospheric pressure. The time-domain IR-LIF model was critical to achieving accurate temperature measurements at 1 kHz due to the LIF signals exiting the steady state regime and no longer tracing the absorption lineshapes.

I. Nomenclature

A_{int}	=	integrated absorbance of an absorption transition
E"	=	lower-state energy of an absorption transition
FQY	=	fluorescence quantum yield
L	=	path length through imaged volume
P	=	optical power
P_i	=	partial pressure of absorbing species
S	=	absorption transition linestrength
S_F	=	LIF signal
T	=	gas temperature
α	=	spectral absorbance
$\Delta\nu_c$	=	collisional full-width at half-maximum
η	=	collection efficiency
ν	=	optical frequency
ν_o	=	transition linecenter frequency
τ_{decay}	=	characteristic time for LIF signal to decay
τ_{ss}	=	characteristic time for LIF signal to reach steady state
ϕ	=	absorption transition lineshape

II. Introduction

Infrared laser-induced fluorescence (IR-LIF) offers the potential to provide spatially resolved measurements of gas properties and countless molecular species. This is because IR-LIF relies on pumping rovibrational transitions

*Former Postdoctoral Research Associate, School of Mechanical Engineering, 585 Purdue Mall, West Lafayette, IN 47907
Postdoctoral Researcher, Mechanical Engineering, University of Colorado, Boulder, CO
†Graduate Student, School of Aeronautics and Astronautics, 701 W Stadium Ave, West Lafayette, IN 47907
‡Associate Professor, School of Mechanical Engineering, 585 Purdue Mall, West Lafayette, IN 47907, AIAA Senior Member

and detecting the ensuing infrared fluorescence, thereby making it applicable, in principle, to all molecules except homonuclear diatomics. That being said, the limited availability of high-power infrared light sources has limited the development of such diagnostics since the early pioneering work of Kirby and Hanson who focused on imaging CO and CO_2 using pulsed lasers [1–3].

Recently, several high-power wavelength-tunable infrared light sources have become available (e.g., quantum-cascade lasers and novel optical parameteric oscillators) which has enabled the development of a new generation of continuous-wave scanned-wavelength IR-LIF diagnostics. For example, Goldenstein et al. [4] demonstrated a QCL-based IR-LIF diagnostic for point measurements of gas temperature, pressure, and CO_2 at up to 100 Hz. However, the measurements were limited to ambient temperature. More recently, Mathews et al. [5] demonstrated the first use of a wavelength-tunable continuous-wave optical parameteric oscillator for performing IR-PLIF imaging of CO_2 in a heated jet, but the measurements were limited to a rate of 10 Hz. In addition, Mathews and Goldenstein [6] demonstrated the first wavelength-modulated infrared planar laser-induced-fluorescence diagnostic for background-free imaging of CO in CO-H_2 diffusion flames. However, only qualitative imaging of CO was demonstrated.

Here we present the initial development and application of the first IR-LIF temperature diagnostic based on CO and the first IR-LIF thermometer demonstrated at high temperatures and in combustion gas. Equally importantly we present the first IR-LIF diagnostic capable of providing measurements at 1 kHz, which represents a 10x improvement upon prior continuous-wave IR-LIF diagnostics and a 100x improvement over pulsed-laser-based IR-LIF diagnostics. These advancements were made possible through the use of a dual-band excitation scheme employing a distributed-feedback (DFB) QCL emitting near 5 μm and a wavelength-tunable OPO emitting near 2.3 μm as well as a novel time-domain model for scanned-wavelength LIF signals.

III. Fundamentals of Laser-Induced Fluorescence

In LIF, laser light resonant with an absorption transition of the target species is used to pump molecules into an excited state where the molecules can undergo spontaneous emission (i.e., fluorescence). At steady state, the LIF signal emanating from an optically thin volume, S_F, is given by Eq. 1.

$$S_F(\nu) = P(\nu) \times \alpha(\nu) \times \mathrm{FQY} \times \eta \tag{1}$$

Here, P is the laser power which depends on optical frequency ν, α is the spectral absorbance, FQY is the fluorescence quantum yield, and η is the fraction of emitted photons that are collected by the imaging system. The spectral absorbance is given by Eq. 2.

$$\alpha(\nu) = S(T) P_i \phi(\nu) L \tag{2}$$

Here, S is the transition linestrength, P_i is the partial pressure of the absorbing species, ϕ is the transition lineshape function and L is the length of the volume of gas from which LIF signal is collected.

Typically, LIF measurements are performed using high-power fixed-wavelength light sources in order to maximize the LIF signal. Here, however, scanned-wavelength LIF measurements are performed in order to effectively image LIF signals that trace, or nearly trace, the lineshape of the absorption transition within the volume being imaged. In doing so, the transition-integrated LIF signal for a given absorption transition can be determined, thereby enabling quantitative calibration-free temperature measurements to be performed analogous to conventional two-color laser absorption techniques, but with the spatial resolution of an LIF measurement.

IV. Experimental Procedures

A. Experimental Setup

Figure 1 shows a schematic of the experimental setup used to perform dual-band scanned-wavelength IR-LIF temperature measurements. The QCL and seed laser of the OPO were injection-current tuned with alternating sawtooth waveforms produced by an arbitrary function generator to sequentially scan the wavelength of each light source across absorption transitions of CO. The waveforms were 180 degrees out of phase to ensure that only one light source was scanning across a CO absorption transition at a given moment in time. The QCL and OPO seed laser were injection-current tuned at either 100 Hz or 1 kHz. The QCL scanned across the P(0,30) transition of CO near 2013.3 cm^{-1} with an optical power near 141 mW. The OPO scanned across the R(0,10) transition of CO near 4297.7 cm^{-1} with

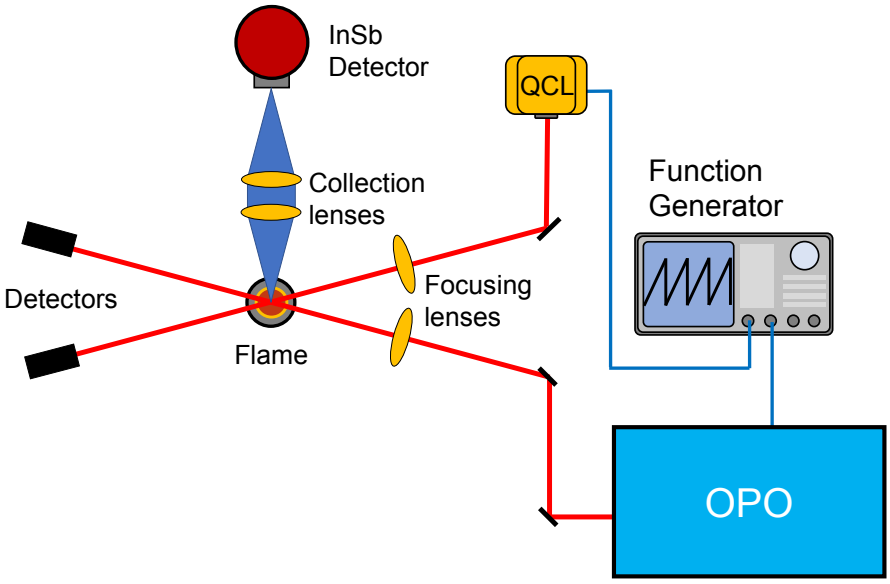

Fig. 1 Experimental setup used to perform IR-LIF temperature measurements of CO in a CO-H_2-Ar diffusion flame burning in air at atmospheric pressure.

an optical power near 1.87 W. These transitions were targeted due to their disparate lower-state energies (E"=1783 cm^{-1} for the P(0,30) and E"=211.4 cm^{-1} for the R(0,10) transition) and favorable linestrengths at the conditions of interest. Notably, the higher power OPO targeted an overtone band transition while the lower power QCL targeted a fundamental band transition. This configuration enabled comparable LIF signal magnitudes to be produced by each light source despite an order of magnitude difference in optical power. Further, prohibitively large absorption was avoided by using the OPO to pump a low-E" overtone band transition.

Each beam was focused with a 75 mm focal length CaF_2 lens to a $1/e^2$ diameter of approximately 0.53 mm and 0.2 mm for the QCL and OPO, respectively. The beams crossed along the centerline of a diffusion flame produced from a 49/2/49 mixture of CO/H_2/Ar. The burner was placed on a vertical translation stage to vary the beam height from 0.1 to 20 mm above the burner. The LIF signal emanating from the crossing point was collected and focused onto an LN_2-cooled InSb detector using a lens doublet consisting of two 25 mm focal length 25.4 mm diameter CaF_2 lenses. The InSb detector's voltage signal was recorded on a 10-bit oscilloscope at a rate of 1 MS/s. Reference measurements of the QCL and OPO intensity were recorded with photodiode detectors to account for variation in optical power across the wavelength scan, which alters the shape of the LIF signal. A solid germanium etalon was used to characterize the wavelength scanning of the QCL and OPO.

B. Data Processing

The relative magnitude of integrated absorbances of each transition was determined using a nonlinear fitting routine to fit simulated LIF signals to the measured LIF signals. LIF signals for each transition were simulated in the time domain as a function of the characteristic LIF steady state time (τ_{ss}), characteristic LIF decay time (τ_{decay}), integrated absorbance (A_{int}), absorption linecenter frequency (ν_0), and collisional-broadening full width at half maximum ($\Delta\nu_c$) assuming a Voigt lineshape profile. Simulated LIF signals were compared to measured LIF signals in the time domain, and the free parameters were varied following a Levenberg-Marquardt algorithm until the simulation converged to a best-fit solution yielding the integrated area of each transition. The ratio of integrated areas was then used to calculate the gas temperature following a standard two-color thermometry technique and assuming an equal FQY for each transition. By performing spectral fitting of LIF signals in the time domain, the spectroscopic parameters of each absorption transition (i.e., A_{int}, ν_0, $\Delta\nu_c$) could be extracted from the measured LIF signals despite apparent distortion of the absorption lineshapes due to the finite rates of LIF excitation and decay. Furthermore, prior knowledge of τ_{ss} and τ_{decay} was not required because they were free parameters of the time-domain LIF model.

LIF signals produced from one scan of the QCL and one scan of the OPO were simulated and fit to measured data

simultaneously to provide a time-resolved measurement at the scan rate of the lasers. For each scan, the LIF signals were simulated as follows: (1) the steady-state LIF signal for each transition was calculated as a function of time, (2) the time-dependent LIF signal for each transition was simulated at each time step in the scan, (3) the LIF contributions from each transition were added together. The steady-state LIF signal for each transition was calculated using Eq. 1, where measured values of the time-varying laser power, $P(t)$, and optical frequency, $\nu(t)$, were used to provide a time-domain, steady-state LIF signal. The time-dependent LIF signal from each transition was calculated assuming its value was driven towards the steady state LIF value at a rate proportional to the difference between the time-dependent and steady-state LIF signals. The proportionality constant was either the inverse of τ_{ss} or τ_{decay} if the time-domain signal was less than or greater than the steady state signal, respectively. The time-dependent LIF signal was initially set equal to the steady state value, and the forward Euler method was used to calculate the time-dependent LIF signal at each subsequent time step with a discrete time resolution defined by the inverse of the data acquisition rate.

V. Results

Figure 2 shows measured LIF signals and resulting best-fit LIF signals at laser scan rates of 100 Hz (left) and 1 kHz (right) acquired approximately 0.1 mm above the burner surface. For each case, the first LIF signal is produced by excitation with the QCL, and the second LIF signal is produced by excitation with the OPO. The LIF signals measured at a scan rate of 100 Hz do not exhibit significant asymmetry indicating that the LIF signal stays in the steady state regime throughout the scan and therefore trace the local absorption lineshapes. In this limit, a frequency-domain fit using a Voigt profile produces similar results to a time-domain fit. In contrast, the LIF signals measured at a scan rate of 1 kHz exhibit significant asymmetry due to the fact that both light sources are scanned across the absorption transitions too fast for the LIF signal to stay in the steady state regime. This is further supported by the reduced magnitude of the LIF signals when scanning at 1 kHz. As a result, the time-domain model is required to accurately model the measured LIF signals, and this approach led to excellent agreement between measured and best-fit LIF signals. In addition, the measurements acquired at 100 Hz and 1 kHz indicate that the gas temperature is nearly the same, differing by only 2.4 K. These results support the accuracy of the time-domain model.

Figure 3 shows example measurements of temperature time histories acquired at scan rates of 100 Hz and 1 kHz at a height of approximately 0.1 mm above the burner surface. The mean gas temperature is similar for both measurement rates. More specifically, it is 378.7 K for the 100 Hz measurements and 367.8 K for the 1 kHz measurements. In

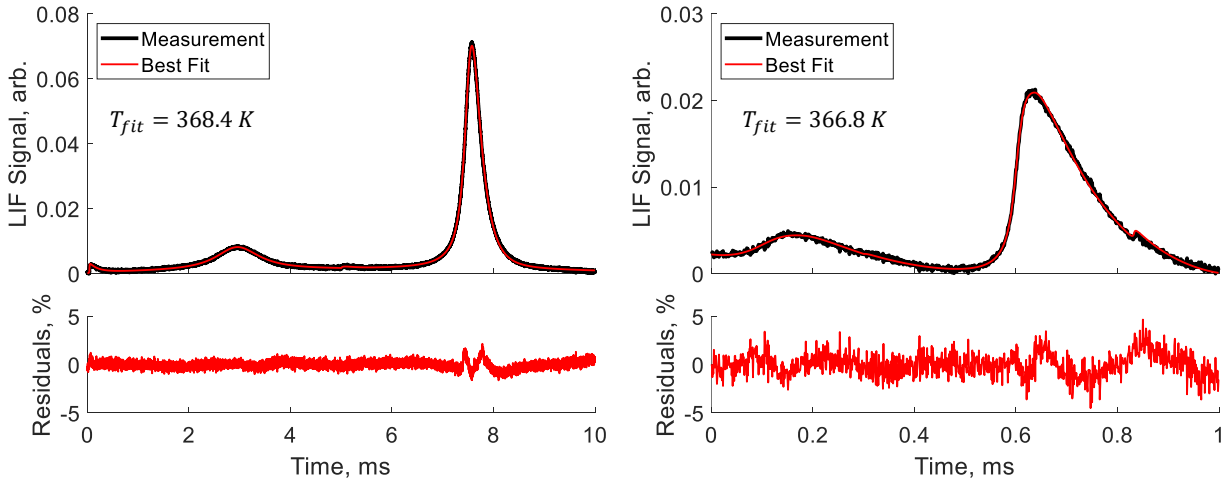

Fig. 2 Measured LIF signals and resulting best-fit LIF signals for measurements performed with laser scan rates of 100 Hz (left) and 1 kHz (right).

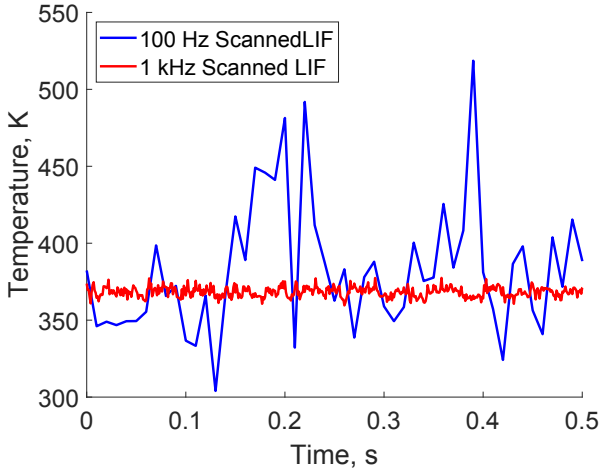

Fig. 3 Temperature time histories measured at 0.1 mm above the burner at rates of 100 Hz and 1 kHz using the scanned-wavelength IR-LIF diagnostic.

CO-H_2-Ar diffusion flame with a measurement rate of 100 Hz or 1 kHz. The average values of temperatures measured over a one second duration are reported, and the error bars show one standard deviation from the mean value. The measurements acquired at rates of 100 Hz and 1 kHz agree within the measurement precision at all measurement locations. This further supports the accuracy of the time-domain model and its ability to accurately recover the integrated LIF signal corresponding to each transition despite operating outside the steady-state regime. The measurements acquired at 1 kHz exhibit significantly smaller measurement precision at all locations for the same reasons mentioned previously.

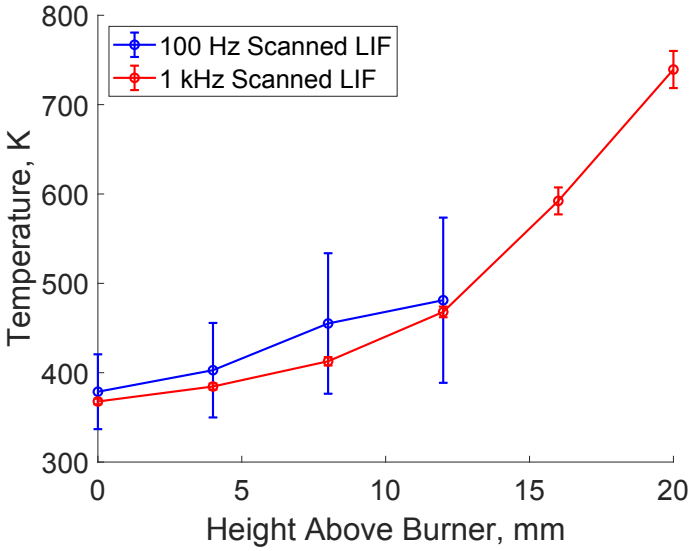

Fig. 4 Time-averaged gas temperature measured at rates of 100 Hz and 1 kHz at the center of a CO-H_2-Ar diffusion flame at different heights above the burner.

VI. Conclusions

This work presented the development and initial application of the first two-color IR-LIF temperature diagnostic. Further, the diagnostic presented here can provide scanned-wavelength IR-LIF measurements at rates up to 1 kHz which represents a 10x increase in measurement rate over previously developed scanned-wavelength IR-LIF diagnostics and a 100x increase in measurement rate over pulsed IR-LIF diagnostics. The advancements reported here were achieved by (1) using a novel dual-band excitation scheme and (2) developing a time-domain IR-LIF model to enable gas properties to be extracted from scanned-wavelength IR-LIF signals produced with high scan rates where the LIF signal does not stay within the steady state regime.

Temperature measurements were presented at rates of 100 Hz and 1 kHz in a CO-H_2-Ar diffusion flame burning in air at atmospheric pressure. The measurements agreed well with each other, thereby supporting the accuracy of the time-domain LIF model. In addition, the 1 kHz measurements exhibited a superior measurement precision, often below 1% of the mean temperature, thereby illustrating the value of using kHz scan rates and its potential for providing high-fidelity measurements of gas temperature.

The work presented here illustrates several critical advancements that demonstrate, for the first time, the potential of IR-LIF to characterize transient flows and flames with kHz measurements. Future research remains needed to (1) improve measurement rates even further, (2) improve measurement sensitivity, (3) expand the measurement capabilities of IR-LIF, and (4) to develop similar IR-LIF diagnostics for a wide range of species that are not well suited for conventional ultraviolet LIF techniques.

Acknowledgments

This work was supported by NSF CBET CAREER Award 1847464.

References

[1] Kirby, B. J., and Hanson, R. K., "Planar laser-induced fluorescence imaging of carbon monoxide using vibrational (infrared) transitions," *Applied Physics B*, Vol. 69, 1999, pp. 505–507.

[2] Kirby, B. J., and Hanson, R. K., "Imaging of CO and CO_2 using infrared planar laser-induced fluorescence," *Proceedings of the Combustion Institute*, Vol. 28, 2000, pp. 253–259.

[3] Kirby, B. J., and Hanson, R. K., "CO_2 imaging with saturated planar laser-induced vibrational fluorescence." *Applied Optics*, Vol. 40, 2001, pp. 6136–6144.

[4] Goldenstein, C. S., Miller, V. A., and Hanson, R. K., "Infrared planar laser-induced fluorescence with a CW quantum-cascade laser for spatially resolved CO_2 and gas properties," *Applied Physics B*, Vol. 120, No. 2, 2015, pp. 185–199.

[5] Mathews, G. C., Stiborek, J. W., and Goldenstein, C. S., "Infrared laser-induced fluorescence with a continuous-wave optical parametric oscillator," *CLEO*, 2021, pp. 1–2.

[6] Mathews, G. C., and Goldenstein, C. S., "Wavelength-modulated planar laser-induced fluorescence for imaging gases," *Optics Letters*, Vol. 42, No. 24, 2017, pp. 5278–5281.